Research Article GU J Sci, Part A, 11(4): 676-689 (2024) 10.54287/gujsa.1537785

Gazi University
Journal of Science
PART A: ENGINEERING AND INNOVATION
http://dergipark.org.tr/gujsa

Evaluating the Impact of Edge-Seal on the Performance of Double-Glass Solar Photovoltaic Modules

Melikenur GENC[1] Abdulkerim GOK[2*]

[1] *Department of Chemical Engineering, Gebze Technical University, Gebze/Kocaeli, Türkiye*
[2] *Department of Materials Science and Engineering, Gebze Technical University, Gebze/Kocaeli, Türkiye*

Keywords

PV Modules
Encapsulants
Edge-seal
Moisture-ingress
Damp Heat
Degradation

Abstract

Solar energy is a vital component of the renewable energy landscape. Nevertheless, photovoltaic (PV) modules face numerous challenges during operation due to environmental stress factors, which can lead to various degradation issues such as delamination, encapsulant discoloration, corrosion of cell metallization, and potential-induced degradation. Ethylene-vinyl acetate (EVA), despite being a prominent encapsulant material, is notably vulnerable to moisture. Upon degradation, EVA releases acetic acid, severely impacting the long-term performance of PV modules. This study investigates the effectiveness of using a polyisobutylene-based edge-seal to minimize moisture ingress in double-glass modules. One-cell mini-modules encapsulated with EVA, with and without edge-seal, are subjected to damp heat testing (85°C / 85% RH) for up to 5000 hours and their performance are evaluated though current-voltage characteristics. Mini-modules without edge-seal exhibit a significant 70% loss in power, primarily due to a 37% decrease in short-circuit current, a 56% decrease in fill factor, and a staggering 650% increase in series resistance. However, mini-modules with edge-seal see only a 33% loss in power, driven mainly by a 21% decrease in fill factor and a 76% increase in series resistance. The use of edge-seal does not completely prevent but effectively reduces moisture ingress and mitigates its detrimental effects on module performance. Additionally, the Network Structural Equation Modeling approach is applied to analyze current-voltage characteristics, enabling the identification of statistically significant relationships, the construction of degradation pathway diagrams, and the determination of key factors contributing to power degradation. This analysis reveals increased series resistance and reduced fill factor as primary causes of power degradation for both mini-module configurations. Although the encapsulant materials exhibit minimal degradation in optical, chemical, and thermo-chemical properties, the presence of moisture within the module construction can still cause corrosion of cell metallization. This results in a decline in power performance even without substantial acetic acid formation. This study highlights the critical importance of preventing moisture ingress to enhance the durability and reliability of PV modules, ensuring their optimal performance throughout their intended service lifetime.

Cite

Genc, M., & Gok, A. (2024). Evaluating the Impact of Edge-Seal on the Performance of Double-Glass Solar Photovoltaic Modules. *GU J Sci, Part A, 11*(4), 676-689. doi:10.54287/gujsa.1537785

Author ID (ORCID Number)

0009-0005-0350-8664 Melikenur GENC
0000-0003-3433-7106 Abdulkerim GOK

Article Process

Submission Date 23.08.2024
Revision Date 19.09.2024
Accepted Date 07.10.2024
Published Date 30.12.2024

1. INTRODUCTION

Historically, energy production has depended heavily on cost-effective but environmentally harmful fossil fuels. This dependence is increasingly seen as unsustainable due to the environmental damage caused and the finite nature of these resources. In response, renewable energy is promoted through policies and incentives aimed at achieving net-zero emissions. Photovoltaics (PV) have become a leading technology in the shift towards sustainable energy. Utilizing sunlight to generate clean electricity is now widely recognized as a promising solution. Over the past decade, the global installed capacity of PV systems has seen remarkable growth. It reached 1.2 TW in 2022 (IEA PVPS, 2023), expanded to 1.6 TW in 2023 with the addition of approximately 400 GW (IEA PVPS, 2024), and is projected to surpass 2 TW in 2024 (BNEF, 2024). While

*Corresponding Author, e-mail: agok@gtu.edu.tr

the future of PV installations looks promising, challenges related to the durability and reliability of PV modules still need addressing to ensure their long-term performance (Aghaei et al., 2022). These issues must be targeted to maintain sustainable growth in the renewable energy sector.

PV modules are composed of several key components, each playing a crucial role in ensuring efficiency, durability, reliability, and long-term performance. At the core are solar cells, typically made from mono-crystalline silicon, which harness sunlight and convert it into electricity through the photovoltaic effect. These cells are protected by a front glass cover, tempered to enhance durability and minimize reflectivity, allowing maximum light transmission. Surrounding the cells is an encapsulant which provides structural support for mechanical stability, enhances optical coupling, ensures electrical isolation for safety and prevents leakage currents, and provides protection against environmental conditions (Czanderna & Pern, 1996). It also plays a crucial role in managing heat distribution across the module's various layers, making high thermal conductivity essential for reduced cell temperatures and optimal performance. The polymeric backsheet further isolates and protects the module from environmental stressors and provides electrical insulation. An aluminum frame offers structural support and facilitates mounting, while a junction box houses electrical connections along with bypass and blocking diodes. Additionally, an anti-reflective coating is applied to the cells and/or glass cover to increase light absorption.

In recent years, especially after the development of bifacial solar cell technology, the polymeric backsheet film has been replaced with another glass layer. According to International Technology Roadmap for Photovoltaics, double-glass modules captured nearly 40% of the market in 2023 and are projected to dominate with over 70% market share by 2034 (ITRPV, 2024). They offer several advantages over traditional modules with polymeric backsheets (Sinha et al., 2021). The double-glass construction enhances durability, providing better protection against environmental factors, thereby improving the service lifetime of PV modules. This construction also increases mechanical strength, making the modules more resistant to mechanical stresses, and improves fire resistance as glass is fire-resistant compared to polymeric materials. Additionally, double-glass modules maintain a more stable aesthetic and performance over time as glass is less prone to discoloration and degradation. These modules are usually designed as bifacial, capturing light from both sides to boost energy yield, particularly in reflective grounds. Furthermore, they exhibit improved resistance to Potential-Induced Degradation (PID), enhancing reliability and performance. From an environmental perspective, double-glass modules are more sustainable as they are easier to recycle at the end of their life cycle compared to modules with polymeric backsheets, which are made of multi-layer films typically consisting of fluoropolymers (Müller et al., 2021). While they may come with higher initial costs, specifically due to increased weight affecting transportation costs, the long-term benefits make double-glass modules more preferable.

During operation in open-air climates, PV modules face a variety of environmental stress factors that can impact their performance and experience degradation and failure (Köntges et al., 2014; 2017). Prolonged exposure to UV radiation can degrade the polymeric encapsulant and backsheet layers, resulting in discoloration. This degradation, especially the discoloration of the encapsulant, can diminish light transmission, decreasing the amount of light that reaches the cells and consequently lowering energy output. While discoloration may initially appear to be an aesthetic issue, it often indicates deeper problems with the polymeric components. It can signal potential delamination between layers, forming gaps where moisture and contaminants can enter, further compromising the module’s integrity. Moisture from rain, snow, and humidity can lead to water ingress, causing corrosion of cell metallization, increased series resistance, and reduced performance. It can react with polymeric materials through hydrolysis, compromising their functionality. High winds can impose mechanical stress on the module's mounting structures, while hail and impact damage can generate physical defects on the surface and cell cracks. Accumulation of dust and debris can block light, reducing energy output, and airborne pollutants can cause material degradation. In coastal areas, saline environments can accelerate corrosion reactions. Additionally, repeated thermal cycling or temperature fluctuations can lead to mechanical stresses, thermal expansion and contraction, material fatigue, and ultimately result in delamination and cell interconnect failures. Addressing these stress factors through robust design and regular maintenance is crucial to ensuring the long-term performance of PV modules.

Ethylene-Vinyl Acetate (EVA) is the most widely used encapsulant material in PV modules, offering numerous benefits (Griffini & Turri, 2016). EVA is a chemically crosslinked, semi-crystalline copolymer made up of

ethylene and vinyl acetate units, usually in a ratio of 70% ethylene to 30% vinyl acetate. Crosslinking agents are added to chemically bond the EVA polymer chains during the lamination process, forming a durable elastomeric network that enhances mechanical strength. EVA's excellent adhesion properties ensure that solar cells remain securely in place, maintaining optimal electrical contact. Its high transparency allows maximum sunlight to reach the cells, which is crucial for achieving high energy conversion efficiency. The material's flexibility and ability to conform to thermal expansion and contraction help minimize the risk of mechanical stress and damage. Additionally, EVA provides electrical insulation, preventing short circuits and ensuring safe operation of the module. EVA is also easy to process during module manufacturing. It can be readily laminated onto solar cells and other layers using standard equipment, streamlining the production process and ensuring consistent quality. Despite these benefits, it does have some significant drawbacks (Oliveira et al., 2018). EVA can degrade over time due to prolonged exposure to environmental conditions, potentially compromising its protective qualities and diminishing module performance. Although EVA is designed to shield cells from moisture, it can still absorb moisture, leading to issues such as corrosion of cell metallization and reduced module performance. EVA's flexibility helps it accommodate thermal expansion and contraction, but it may still experience stress from temperature fluctuations, potentially causing delamination or other damage if not properly managed. While EVA performs adequately across a range of temperatures, it has limitations under extreme conditions. Prolonged high temperatures can diminish its mechanical properties and adhesive strength, while very cold temperatures can make it more brittle, increasing the risk of cracking and affecting durability. Additionally, EVA's production and disposal have environmental implications, as it is not easily recyclable, raising concerns about waste management and sustainability.

When EVA degrades, a key issue is the formation of acetic acid from the breakdown of vinyl acetate (Kempe et al., 2007). This byproduct can accelerate the corrosion of cell metallization, increase series resistance, and ultimately cause power loss. Figure 1 illustrates the degradation reactions that lead to acetic acid formation (Hara & Chiba, 2021). Additionally, acetic acid can affect the adhesion properties of EVA, potentially leading to delamination between the EVA and the front glass or backsheet layers. Degradation by-products that absorb visible light can also cause discoloration, reducing light transmission to the cells. Significant discoloration often signals extensive degradation of the encapsulant. Elevated temperatures can worsen these degradation effects. Residual reactive crosslinking agents, i.e., peroxide species, from the lamination process can further accelerate degradation. Therefore, selecting the right packaging materials, combinations, and lamination processes is crucial for enhancing the durability and reliability of PV modules in various environmental conditions. This approach not only ensures long-term performance but also helps lower the levelized cost of electricity and reduces greenhouse gas emissions, contributing to a more sustainable future (Paç & Gok, 2024).

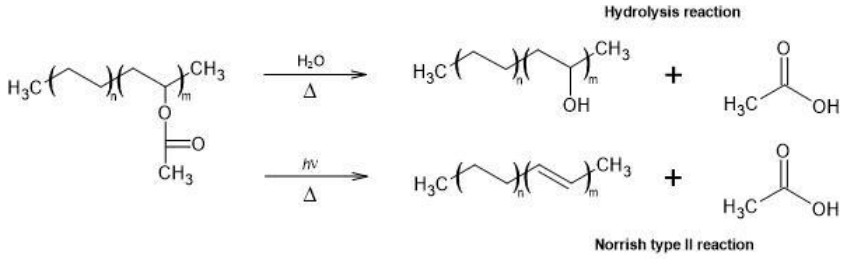

Figure 1. *Acetic acid formation during hydro-thermal and photo-thermal degradation of EVA*

Reported issues with EVA highlight the importance of ongoing research and development to address material limitations and enhance the overall reliability and sustainability of PV modules. There are several alternatives to EVA, each offering unique advantages (Dintcheva et al., 2023). Recent studies have focused especially on Polyolefin Elastomers (POE), Thermoplastic Olefins (TPO), and ionomers (ION) as promising alternatives to traditional EVA encapsulants (Schnatmann et al., 2022). These materials feature a polyethylene backbone but differ from EVA by incorporating side groups such as acrylates, acrylic acids, or n-alkanes instead of EVA's vinyl acetate. This modification addresses a key drawback of EVA: the formation of acetic acid during degradation. In addition, these alternative encapsulants offer improved volume resistivity and lower water vapor transmission rates, presenting significant advantages over EVA. Moreover, physically crosslinked encapsulants can be more readily recyclable, offering notable benefits in terms of sustainability. Nevertheless,

these alternatives typically come with a higher cost than EVA, and as a result, EVA remains the most cost-effective option, offering a good balance between cost and performance.

In double-glass solar modules, both the front and back surfaces are made of glass, which is impermeable to moisture. However, moisture can still penetrate through the edges. To further reduce the risk of moisture ingress, Polyisobutylene (PIB) is commonly used as an edge-seal material (Kempe et al., 2015). A reliable edge-seal is essential for protecting internal components from environmental factors. PIB is highly effective because of its extremely low water vapor permeability, which helps prevent moisture ingress that could cause corrosion, delamination, and decreased module performance. Its strong adhesion to glass and other module materials, along with its flexibility to accommodate thermal expansion and contraction, ensures a secure seal throughout the module's service lifetime. Additionally, PIB's resistance to UV radiation and other environmental stresses preserves its sealing properties, while its ease of application during manufacturing guarantees consistent sealing. These characteristics make PIB a popular and effective choice for edge-seal application in double-glass modules, significantly enhancing their durability and long-term performance.

This study examines the electrical performance of single-cell mini-modules with a double-glass construction, encapsulated with EVA, both with and without edge-seal. The double-glass design enhances the reliability of modules by effectively minimizing moisture ingress, which is crucial for reducing encapsulant material degradation and solar cell metallization corrosion. The edge-seal further enhances this protection, further mitigating the detrimental impacts of moisture on module performance. Formation and accumulation of acetic acid in double-glass modules can be a serious concern due to unbreathable structure. This trapped acetic acid inside the module can accelerate the degradation processes and lead to service lifetime issues. To ensure long-term performance, the modules underwent rigorous reliability testing beyond the IEC 61215 standards (IEC, 2021). The current-voltage (I-V) characteristics of the modules were extensively analyzed and modeled using the Network Structural Equation Modeling approach to identify key factors contributing to power degradation.

2. MATERIALS AND METHOD

To ensure effective module lamination, commercially available EVA encapsulant material was used. To minimize moisture ingress, a double-glass construction was implemented. Mini-modules, each containing a single, bifacial Passivated Emitter Rear Contact (PERC) cell, were laminated using these encapsulants, both with and without PIB-based edge-seal. Each configuration includes two mini-module samples.

The lamination process plays a vital role in PV module manufacturing, as it ensures proper curing of EVA and strong adhesion between layers, which are essential for the durability and reliability of the final product. In this study, mini-modules with EVA encapsulants were laminated at a temperature of 150 °C, beginning with 5 minutes of evacuation to remove air, followed by 10 minutes under a pressure of approximately 900 mbar.

After lamination, the mini-modules underwent damp heat exposure for up to 5000 hours. This test is part of the IEC 61215 standard, which evaluates the long-term performance of PV modules under high temperature and humidity conditions. The protocol involves exposing modules to 85°C and 85% relative humidity for 1000 hours. This test provides crucial insights into potential manufacturing flaws and hydrothermal degradation mechanisms that could occur in real-world operation. Although the standard mandates 1000 hours of testing, this study extended the testing time to 5000 hours to ensure that the module designs meet long-term performance expectations.

To evaluate the electrical characteristics of the mini-modules during damp heat testing, current-voltage (I-V) curve measurements were conducted approximately every 500 hours. I-V curves are essential for characterizing PV module performance, illustrating the relationship between current and voltage at the module's terminals. Typically, these curves are measured under Standard Testing Conditions (STC), which include an irradiance of 1000 W/m², a cell temperature of 25°C, and an air mass of 1.5. A solar simulator is used to mimic sunlight, while an electronic load adjusts the resistance across the module to capture current and voltage data at various points. Key parameters such as short-circuit current (I_{SC}), open-circuit voltage (V_{OC}), fill factor (FF), series resistance (R_S), shunt resistance (R_{SH}), and maximum power point (P_{MP}) are then extracted from the curve.

The Network Structural Equation Modeling (netSEM) approach was then employed to develop degradation pathways, elucidating the relationships between a primary stressor (S), mechanistic (M) variables, and a performance response (R) variable. netSEM extends traditional SEM by integrating non-linear relationships to analyze complex relationships within data and by incorporating network structures to provide a deeper understanding of interconnected systems (Gok et al., 2019). netSEM not only estimates and tests relationships but also visualizes the network structure, highlighting central nodes and influential paths. netSEM explores the most suitable model between univariate relationships by utilizing various linear and non-linear functional forms, encompassing linear, simple quadratic, quadratic, exponential, logarithmic, and change point models. The change point model is the combination of two linear models with changing slopes. Using the step-wise regression approach, all univariate relationships are rank-ordered based on their adjusted R^2 values sequentially and mapped into a degradation pathway diagram to illustrate the relationships among the stressor, mechanistic, and response variables. In these diagrams, arrows indicate relationships between variables, with statistical metrics displayed along the connecting lines. To rank these connections, three adjusted R^2 cutoff values were used: 0.90, 0.60, and 0.30. Strong relationships (adjusted $R^2 \geq 0.90$) are represented by thick solid lines, moderate relationships ($0.90 >$ adjusted $R^2 \geq 0.60$) by standard solid lines, weak relationships ($0.60 >$ adjusted $R^2 \geq 0.30$) by thin solid lines, and negligible relationships (adjusted $R^2 < 0.30$) by thin dotted lines.

Since this method only evaluates univariate relationships, mechanistic multi-step pathways were derived by substituting one mechanistic variable equation into another. For instance, to determine the multi-step path of "S → M → R," the equations for the "S → M" and "M → R" relationships are first obtained, and then "M" in the first model is substituted into the second model to derive the "M"-dependent multi-step path of "S → R." Plotting these mechanistic relationships over the exposure time illustrates how the mechanistic variables influence overall behavior. A quantitative comparison between the direct "S → R" and the multi-step "S → M → R" pathways is conducted using the root mean square error (RMSE) metric.

In this study, testing time was taken as the main stressor as a proxy to damp heat exposure conditions, P_{MP} was determined as the performance level response, and the remaining I-V curve parameters such as I_{SC}, V_{OC}, FF, and R_S were treated as the mechanistic variables. Since V_{OC} parameter is related to the intrinsic quality of solar cells, recombination mechanisms, and dark saturation current, it did not experience any significant degradation over the exposure time, and thus, it was not included in the analysis in order to focus only on the variables that can explain the observed behavior in power performance with exposure time.

3. RESULTS AND DISCUSSION

Mini-modules encapsulated using EVA, both with and without edge seals, were subjected to damp heat exposure for up to 5000 hours. Their I-V characteristics were periodically evaluated at specific time intervals. Table 1 provides an overview, highlighting the normalized initial and final values to reveal the observed changes. Figure 1 illustrates the temporal progression of I-V curves for a representative mini-module from each configuration. It can be seen that mini-modules demonstrated a significant power loss when edge-seal was not applied; however, this loss was notably less severe with the use of edge-seal.

Table 1. *Initial and final I-V characteristics of the mini-modules*

Mini-module	Edge-seal	Exposure Time	P_{MP}	I_{SC}	V_{OC}	FF	R_S
EVA	×	0	1.00	1.00	1.00	1.00	1.00
		5000	0.12	0.44	0.99	0.29	9.64
EVA		0	1.00	1.00	1.00	1.00	1.00
		5000	0.48	0.83	0.99	0.59	3.29
EVA	✓	0	1.00	1.00	1.00	1.00	1.00
		5000	0.77	0.99	0.99	0.78	1.79
EVA		0	1.00	1.00	1.00	1.00	1.00
		5000	0.77	0.98	0.98	0.80	1.74

Upon reviewing Table 1 and Figure 2, it becomes evident that the main contributor to power loss is the decrease in fill factor primarily due to the increase in series resistances. The open-circuit voltage remains stable, which is consistent with expectations since it is linked to the intrinsic quality of solar cells, recombination mechanisms, and dark saturation current. The short-circuit current exhibits a moderate impact on power; discoloration of the encapsulants contributes to loss in I_{SC} by affecting the interaction of light with the solar cells. The most pronounced effect is the reduction in fill factor, which can be attributed to the corrosion of cell metallization caused by moisture ingress. The increased resistance is indicated by changes in the slopes of the I-V curves near the open-circuit voltage. While no significant optical, chemical, or thermo-chemical degradation of the encapsulant materials was observed, moisture ingress into the module construction can still induce corrosion in cell metallization, thereby increasing series resistance and reducing fill factor. These variations in electrical parameters provide critical insights into the behavior of these mini-modules during extended damp heat exposure, offering valuable information for analyzing degradation pathways.

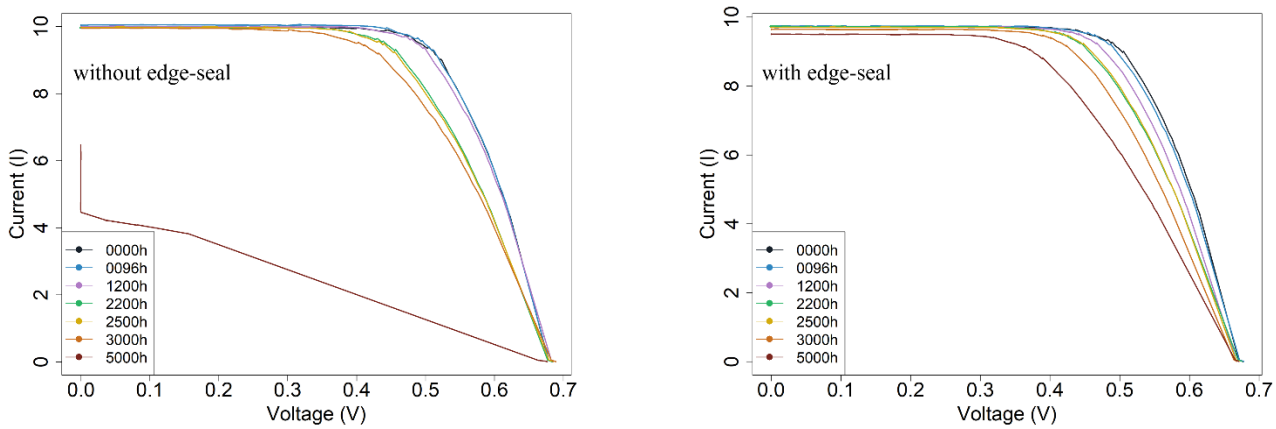

Figure 2. *Temporal evolution of I-V curves of the selected mini-modules under damp heat exposure*

Figure 3 presents the temporal evolution and model predictions of the I-V curve parameters over time (top row), along with the relationship of P_{MP} with these parameters (bottom row) for the mini-modules without edge-seal, using the netSEM approach. Detailed functional forms, goodness-of-fit statistics (adjusted R^2), and model equations are provided in Table 2. The I-V curve parameters exhibit a quadratic trend over time: P_{MP}, I_{SC}, and FF decrease quadratically, while R_S increases. Although the relationship between $P_{MP} \rightarrow I_{SC}$ also follows a quadratic trend, a change point model offers a better fit for the relationships between $P_{MP} \rightarrow$ FF and $P_{MP} \rightarrow R_S$. In these models, the change point is indicated by the value in parentheses followed by the ± sign. Before the change point, the model is represented by the first part of the equation; after the change point, a combined linear equation applies. For instance, the relationship between $P_{MP} \rightarrow$ FF is described by the equation: $-1.232 + 8.788 \cdot FF - 2.066 \cdot (FF - 0.620)$. The change point for FF is 0.620. Before this point, the relationship is linear, represented by $-1.232 + 8.788 \cdot FF$. After this point, the equation becomes $-1.232 + 8.788 \cdot FF - 2.066 \cdot (FF - 0.620)$, which simplifies to $0.049 + 6.722 \cdot FF$. Both the quadratic and change point models suggest an initial induction (damage accumulation) phase followed by a rapid decline in the parameters.

Figure 4 illustrates the degradation pathway diagram for the mini-modules without edge-seal. It appears that the primary factors influencing power performance are FF, R_S, and I_{SC}. This indicates that moisture ingress into the module construction has led to the corrosion of the cell metallization. Although there is a strong relationship between $I_{SC} \rightarrow P_{MP}$, the moderate correlation between Time $\rightarrow I_{SC}$ indicates that significant degradation of the encapsulant is unlikely. While some discoloration was observed, which correlates with P_{MP}, it is not enough to strongly impact I_{SC}. The relationship between the mechanistic variables, such as between $I_{SC} \rightarrow$ FF (or FF $\rightarrow I_{SC}$), FF $\rightarrow R_S$ (or $R_S \rightarrow$ FF), and $I_{SC} \rightarrow R_S$ (or $R_S \rightarrow I_{SC}$) show nearly perfect model fits, highlighting the strong interactions between these parameters. It is important to note that the netSEM analysis explores only statistical correlations; therefore, a strong correlation between two variables does not necessarily imply causation. Expert guidance from domain-specific knowledge is crucial in interpreting the results.

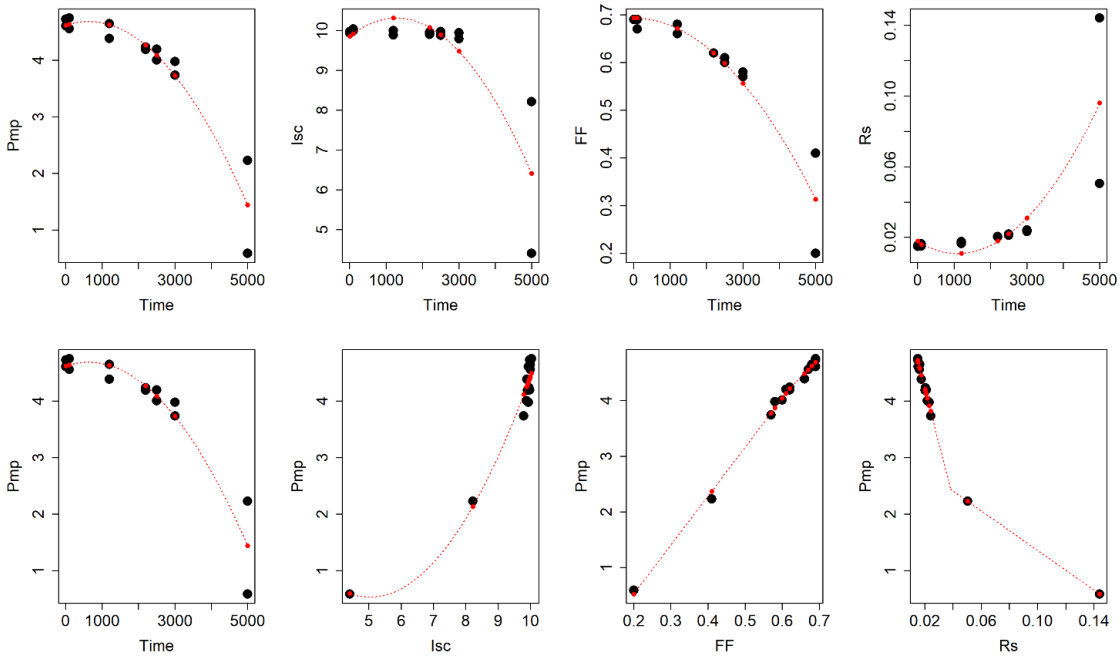

Figure 3. *Model predictions of the I-V curve parameters over time (top row) and model predictions of P_{MP} as a function of I-V curve parameters (bottom row) for the mini-modules without edge-seal*

Table 2. *Model predictions and the corresponding model equations for the selected univariate relationships for the mini-modules without edge-seal*

Path	Model	Adjusted R^2	Model Equation
Time → P_{MP}	Quadratic	0.896	4.623 + 2.120e-04 · Time – 1.696e-07 · $Time^2$
Time → I_{SC}	Quadratic	0.685	9.858 + 7.220e-04 · Time – 2.823e-07 · $Time^2$
Time → FF	Simple Quadratic	0.891	0.693 – 1.519e-08 · $Time^2$
Time → R_S	Quadratic	0.638	1.762e-02 – 1.230e-05 · Time + 5.575e-09 · $Time^2$
Time → P_{MP}	Quadratic	0.896	4.623 + 2.120e-04 · Time – 1.696e-07 · $Time^2$
I_{SC} → P_{MP}	Quadratic	0.949	4.541 – 1.591 · I_{SC} + 0.158 · I_{SC}^2
FF → P_{MP}	Change Point	0.995	-1.232 + 8.788 · FF – 2.066 · (FF-0.620) ±
R_S → P_{MP}	Change Point	0.997	6.180 – 97.494 · R_S + 79.980 · (R_S-0.038) ±

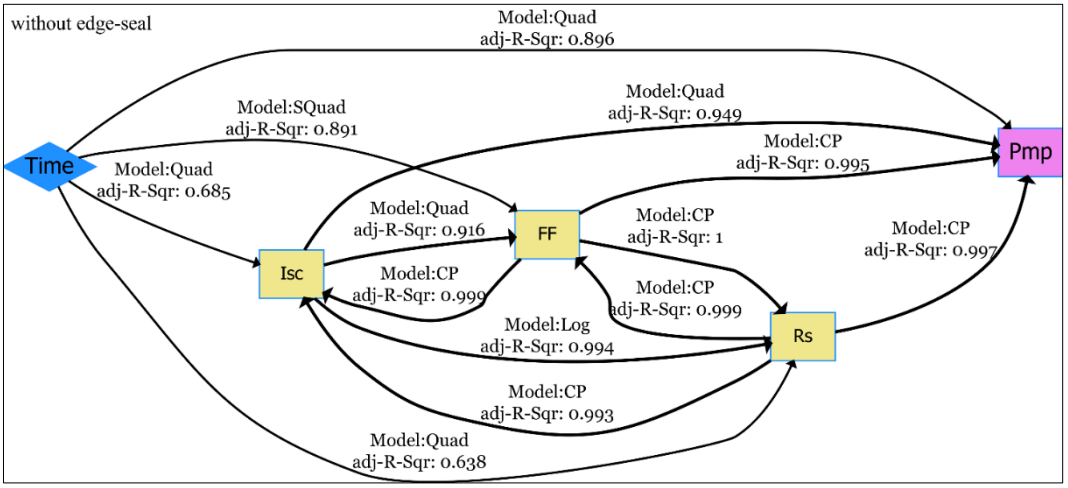

Figure 4. *Degradation pathway diagram for the mini-modules without edge-seal*

Figure 5 compares the direct and mechanistic pathways for the degradation of mini-modules without edge-seal. The direct pathway is represented by the relationship of Time → P_{MP} with an RMSE value of 0.330. Mechanistic pathways include additional variables to this direct pathway. It can be seen that the variation in P_{MP} can be effectively explained by FF with an RMSE value of 0.336, represented by the pathway of Time → FF → P_{MP}. Pathways incorporating R_S and I_{SC} as mechanistic variables also account for the change in P_{MP}, though with slightly higher RMSE values of 0.490 and 0.500, respectively. When considering two mechanistic variables, the combined effect of FF and R_S provides a comprehensive explanation of the observed change in in P_{MP}, resulting in the lowest RMSE value of 0.329, represented by the pathway of Time → FF → R_S → P_{MP}. Although the pathway of Time → R_S → FF → P_{MP} has the highest RMSE value among those with two mechanistic variables, it may better explain the observed change in P_{MP} since exposure increases R_S, which in turn decreases FF. The interplay of three mechanistic variables, namely FF, I_{SC}, and R_S, offers a thorough explanation for the observed variation in P_{MP}. The pathway of Time → FF → I_{SC} → R_S → P_{MP} yields an RMSE value of 0.393, indicating a robust model. Alternatively, the pathway of Time → R_S → I_{SC} → FF → $P_{MP,}$ despite a slightly higher RMSE value, may better reflect the degradation in power due to increased R_S leading to decreased FF. In summary, the decline in FF and power performance can primarily be attributed to moisture-induced reactions, which causes corrosion of cell metallization and discoloration of the EVA encapsulant. For clarity, pathways with more than two mechanistic variables are not shown in Figure 5.

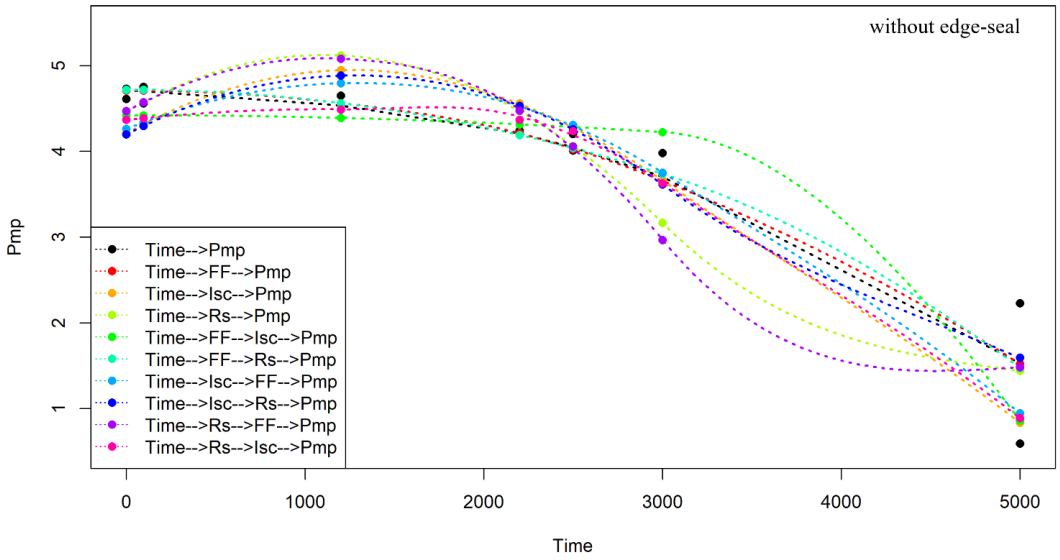

Figure 5. *Comparison of direct and mechanistic pathways for the power degradation of mini-modules without edge-seal*

Figure 6 presents the temporal evolution and model predictions of the I-V curve parameters over time (top row), along with the relationship of P_{MP} with these parameters (bottom row) for the mini-modules with edge-seal, using the netSEM approach. Detailed functional forms, goodness-of-fit statistics (adjusted R^2), and model equations are provided in Table 3. The I-V curve parameters primarily exhibit linear or change point models over time. Although the relationship between Time → I_{SC} has a quadratic nature, the change in I_{SC} over time is minimal, and the data is scattered, resulting in a weak correlation with an adjusted R^2 value of around 0.35. A change point model offers a better fit for the relationships between Time → FF and Time → R_S, but the changes in slopes at the change points are relatively small, appearing mostly simple linear models. The relationships between FF → P_{MP} and R_S → P_{MP} are represented by simple quadratic and simple linear models, respectively. Despite the logarithmic nature of the I_{SC} → P_{MP} relationship, data quality issues result in a modest goodness of fit with an adjusted R^2 value of 0.56.

These findings suggest that the induction (damage accumulation) phase followed by a rapid decline is not observed when the edge-seal is used within the applied exposure time, indicating that degradation progresses slowly due to minimized moisture ingress. It is important to note that moisture ingress involves the diffusion of water molecules into the module construction (Segbefia et al., 2021). This process begins when these molecules are entered into the module and adsorbed onto the surface of the encapsulant. Driven by a

concentration gradient, the molecules then move through the encapsulant and are desorbed onto other components. The diffusion continues until equilibrium is reached with the surrounding humidity. Since relative conditions are constant during damp heat testing, time becomes the most essential factor for this process. In the case of edge-seal, extending the testing time beyond the applied level of 5000 hours could reveal potential nuances and alterations in the observed results, but this may not be feasible due to cost and time constraints.

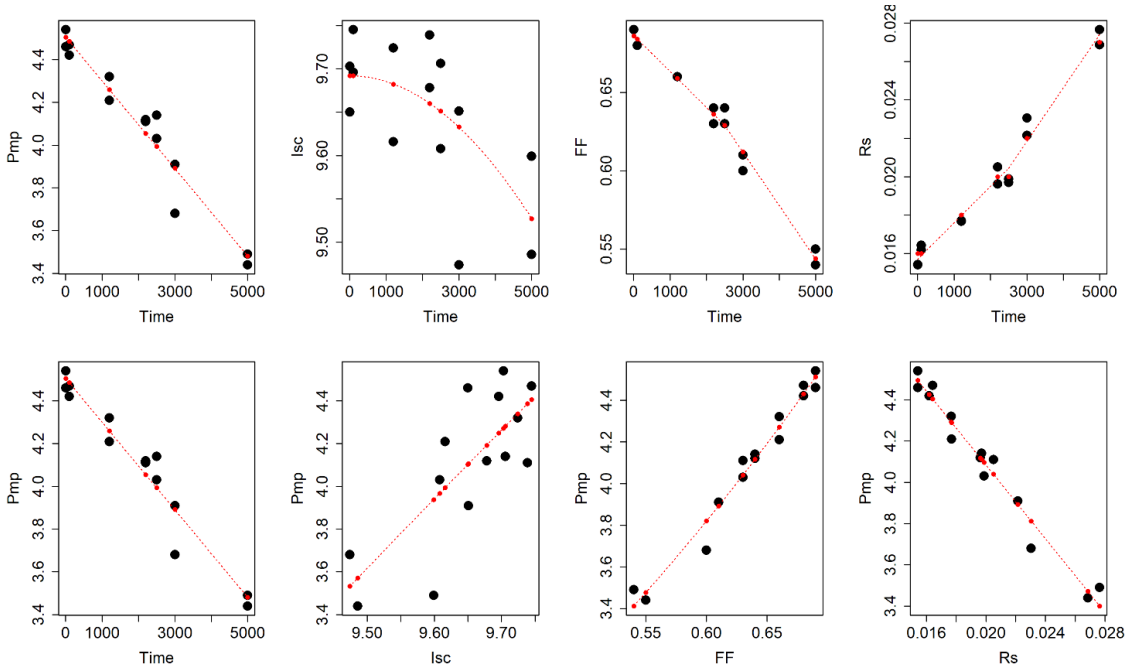

Figure 6. *Model predictions of the I-V curve parameters over time (top row) and model predictions of P_{MP} as a function of I-V curve parameters (bottom row) for the mini-modules with edge-seal*

Figure 7 illustrates the degradation pathway diagram for the mini-modules with edge-seal. The positive impact of using edge-seal is evident here. It appears that the power performance is influenced solely by R_S and FF with no significant effect from I_{SC}. This suggests that encapsulant material degradation is unlikely to be a cause for power loss in this instance. The observed reduction in power performance, though less severe than that in the mini-modules without edge-seal, can still be attributed to moisture ingress and subsequent corrosion of the cell metallization. In this case, the edge-seal did not completely block the entry of moisture, but significantly reduced its extent. Variabilities introduced during the manual lamination and edge-seal application process may also play a role. Given that these mini-modules were assembled manually, these findings highlight the critical importance of maintaining high-quality lamination standards in regular processing conditions. With automated module lamination and edge-seal dispensing, the quality of module construction could be improved, further minimizing moisture ingress.

Table 3. *Model predictions and the corresponding model equations for the selected univariate relationships for the mini-modules with edge-seal*

Path	Model	Adjusted R^2	Model Equation
Time → P_{MP}	Simple Linear	0.940	4.506 – 2.050e-04 · Time
Time → I_{SC}	Simple Quadratic	0.347	9.692 – 6.583e-09 · $Time^2$
Time → FF	Change Point	0.981	0.686 – 2.296e-05 · Time – 1.120e-05 · (Time-2500) ±
Time → R_S	Change Point	0.974	1.570e-02 + 1.899e-06 · Time + 8.881e-07 · (Time-2500) ±
Time → P_{MP}	Simple Linear	0.940	4.506 – 2.050 e-04 · Time
I_{SC} → P_{MP}	Logarithmic	0.564	-66.208 + 31.015 · log(I_{SC})
FF → P_{MP}	Simple Quadratic	0.971	1.674 + 5.960 · FF^2
R_S → P_{MP}	Simple Linear	0.966	5.872 – 89.408 · R_S

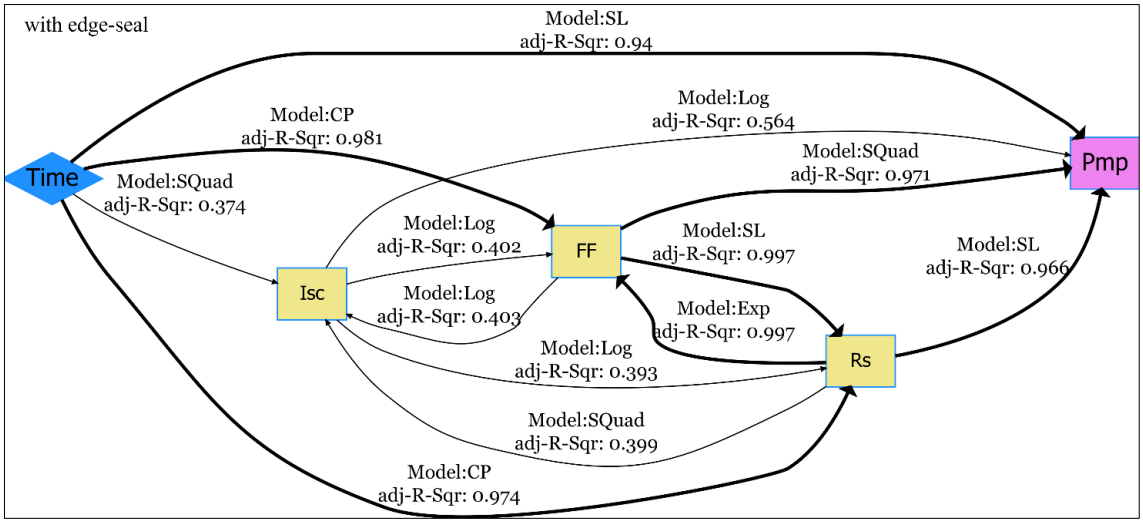

Figure 7. *Degradation pathway diagram for the mini-modules with edge-seal*

Figure 8 compares the direct and mechanistic pathways for the degradation of mini-modules with edge-seal. The direct pathway, represented by the relationship of Time → P_{MP}, has an RMSE value of 0.081. This analysis exhibits similarities to those observed in mini-modules without edge-seal, where variations in P_{MP} are effectively explained through either FF or R_S with RMSE values of 0.075 and 0.078, respectively. In this context, the effect of I_{SC} is relatively minor compared to the other pathways. When considering pathways involving two mechanistic variables, the interaction between R_S and FF provides a more comprehensive explanation of changes in P_{MP}. The pathway of Time → R_S → FF → P_{MP} offers a more integrated approach to understanding power degradation, resulting in the lowest RMSE value of 0.075. Including I_{SC} in this pathway as the third mechanistic variable does not improve the model due to its weak correlation with both Time and P_{MP}, leading to an RMSE value of 0.178.

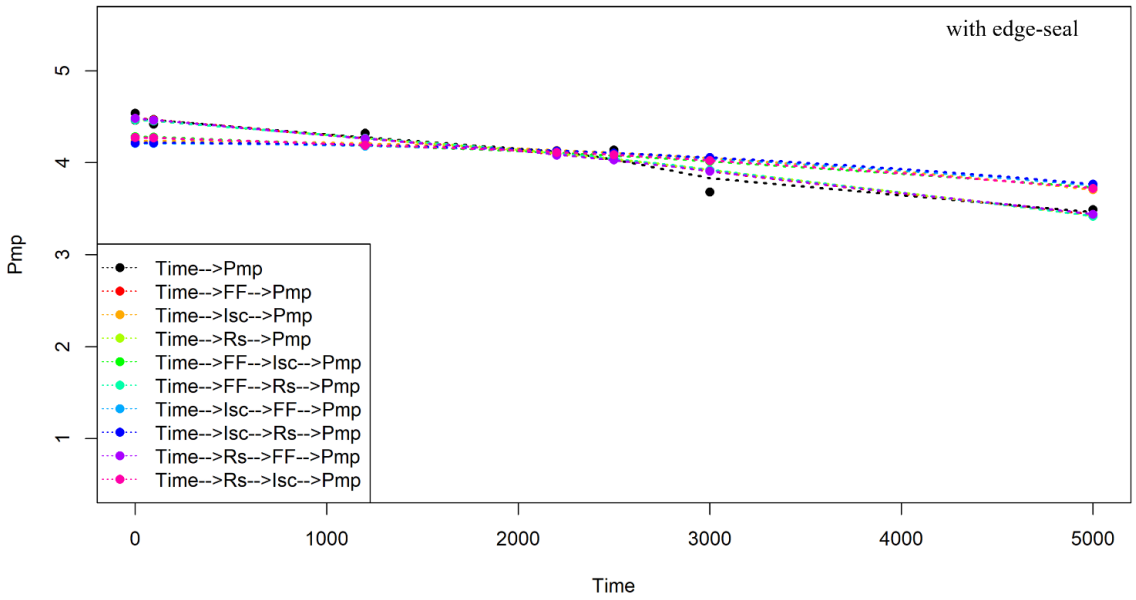

Figure 8. *Comparison of direct and mechanistic pathways for the power degradation of mini-modules with edge-seal*

Comprehensive results detailing the direct and mechanistic degradation pathways are presented in Table 4. In general, the effects of R_S and FF, whether individually or combined, are critical in explaining the observed variations in P_{MP} for both mini-module configurations. To ensure the modules function effectively throughout their service life, protecting against moisture is crucial. Although the use of double-glass construction, replacing the polymeric backsheet, is a useful strategy to minimize moisture ingress, moisture can still

penetrate from the edges. This study explored the critical role of edge-seal application in minimizing moisture ingress and mitigating its detrimental effects on module performance, particularly for designs with moisture-susceptible encapsulant materials like EVA. Mini-modules without edge-seal experienced a substantial 70% loss in power, primarily caused by a 37% reduction in I_{SC}, a 56% decline in FF, and an astonishing 650% rise in R_S. In contrast, mini-modules with edge-seal showed only a 33% loss in power, mainly attributed to a 21% decrease in FF and a 76% increase in R_S. While the edge-seal did not entirely prevent moisture ingress, it minimized its extent, slowed down the degradation, and thus significantly mitigated its impact. While the encapsulant materials showed minimal degradation in their optical, chemical, and thermo-chemical properties, the presence of moisture within the module construction could still lead to corrosion of the cell metallization. This, in turn, impacts power performance, even without significant acetic acid formation.

Table 4. *RMSE values of estimated direct and mechanistic degradation pathways*

		Without edge-seal	**With edge-seal**
Length	**Pathway**	**RMSE**	
0	Time → P_{MP}	0.330	0.081
1	Time → FF → P_{MP}	0.336	0.075
1	Time → I_{SC} → P_{MP}	0.500	0.193
1	Time → R_S → P_{MP}	0.490	0.078
2	Time → FF → I_{SC} → P_{MP}	0.437	0.178
2	Time → FF → R_S → P_{MP}	0.329	0.078
2	Time → I_{SC} → FF → P_{MP}	0.452	0.211
2	Time → I_{SC} → R_S → P_{MP}	0.452	0.214
2	Time → R_S → FF → P_{MP}	0.529	0.075
2	Time → R_S → I_{SC} → P_{MP}	0.424	0.180
3	Time → FF → I_{SC} → R_S → P_{MP}	0.393	0.202
3	Time → FF → R_S → I_{SC} → P_{MP}	0.404	0.180
3	Time → I_{SC} → FF → R_S → P_{MP}	0.452	0.213
3	Time → I_{SC} → R_S → FF → P_{MP}	0.459	0.213
3	Time → R_S → FF → I_{SC} → P_{MP}	0.439	0.178
3	Time → R_S → I_{SC} → FF → P_{MP}	0.402	0.201

To explore the effects of encapsulant type on degradation, it is essential to understand the interaction between polymers and water (Mitterhofer et al., 2020). Water's polar structure enhances chemical interactions with the polymer, especially if the polymer is also polar, facilitating faster moisture transmission. The hydrophilic nature of vinyl acetate groups makes EVA more susceptible to moisture, leading to easy hydrolysis and acetic acid formation, which accelerates degradation. EVA's polar structure allows moisture to diffuse more rapidly compared to non-polar polymers such as polyolefins. Properties of encapsulant materials, such as chemical and network structure, crystallinity, polarity, free volume, crosslinking degree, and volume resistivity, also play a critical role. Determining all these parameters is challenging and beyond the scope of this study. However, some inferences can be made based on the typical properties of encapsulant materials (Oreski et al., 2021) provided in Table 5. Among these, water vapor transmission rate (WVTR) and volume resistivity are significantly important, as WVTR relates to moisture absorption resistance and volume resistivity relates to ion transport resistance and thus PID. EVA has relatively higher WVTR and lower volume resistivity than relatively newer encapsulant materials such as POE and TPO, making it an unfavorable choice, especially for double-glass modules. Although this study investigated only hydro-thermal degradation, photo-thermal degradation also causes acetic acid formation through Norrish II type reactions, as depicted in Figure 1. When double-glass module construction is equipped with impermeable edge-seal, and acetic acid is formed through photo-thermal degradation, it will be trapped inside and accumulate, leading to faster corrosion of cell metallization and accelerated power degradation (Patel et al., 2020). Therefore, if EVA is used for double-glass module construction, it should be used with caution, and strong stabilization against UV radiation becomes essential.

Table 5. *Typical properties of encapsulant materials*

Encapsulant Material	Polymer Type	Glass Transition Temperature	Elastic Modulus	Refractive Index	Volume Resistivity	Water Vapor Transmission Rate
		T_G [°C]	E [MPa]	n	ρ [Ω·cm]	WVTR [g/m^2/day]
EVA	Elastomer	–40 to –34	≤ 68	1.49	10^{14}	34
POE		–50 to –40	≤ 30	1.49	10^{15} to 10^{16}	3.30
PDMS		≤ –100	≤ 10	1.38 to 1.58	10^{14} to 10^{15}	130 to 200
PVB	Thermoplastic	+12 to +20	≤ 11	1.48	10^{10} to 10^{12}	40.05
Ionomer		+40 to +50	≤ 300	1.49	10^{16}	0.19
TPO	Thermoplastic elastomer	–60 to –40	≤ 32	1.48	10^{14} to 10^{18}	2.85

4. CONCLUSION

Solar energy plays a crucial role in the renewable energy sector, yet PV modules and systems encounter numerous operational challenges due to environmental stresses. These stresses can lead to various forms of degradation, compromising the long-term performance and service lifetime of PV modules. While EVA is a widely used encapsulant in PV modules, it is highly susceptible to moisture. As EVA degrades hydrolytically, it releases acetic acid, leading to corrosion of the cell metallization and performance loss. This study explored the use of a PIB-based edge-seal to reduce moisture ingress in double-glass PV modules. One-cell mini-modules encapsulated with EVA, both with and without edge-seal, were subjected to damp heat testing for up to 5000 hours. Mini-modules without edge-seal suffered a 70% loss in power. In contrast, mini-modules with the edge-seal experienced only a 33% power loss. Although the edge-seal did not fully eliminate moisture ingress, it significantly mitigated its effects. Although the encapsulant materials showed minimal degradation, moisture ingress still led to cell metallization corrosion, resulting in degradation in power even without significant acetic acid formation. Additionally, the netSEM approach was applied to analyze the I-V characteristics, allowing for the identification of statistically significant relationships and the construction of degradation pathway diagrams. This analysis confirmed that increased series resistance and decreased fill factor were the main contributors to loss in power in both module configurations. This study underscores the vital importance of preventing moisture ingress to enhance the durability and reliability of PV modules, thereby ensuring their optimal performance throughout their intended service lifetime.

AUTHOR CONTRIBUTIONS

Conceptualization, A.G.; methodology, A.G.; software, A.G. and M.G.; validation, A.G.; formal analysis, A.G. and M.G.; research, A.G. and M.G.; sources, A.G.; data curation, A.G. and M.G.; manuscript-original draft, A.G. and M.G.; manuscript-review and editing, A.G.; visualization, A.G. and M.G.; supervision, A.G.; project management, A.G.; funding, A.G. All authors have read and legally accepted the final version of the article published in the journal.

ACKNOWLEDGEMENT

This study was conducted as part of the Solar-Era.NET project: PV40+ and supported by the funding from The Scientific and Technological Research Council of Turkey (TUBITAK) under the Grant No: 120N520. The authors would like to thank PV40+ project partners for the experimental work and providing data for the analyses conducted in this study.

CONFLICT OF INTEREST

The authors declare no conflict of interest.

REFERENCES

Aghaei, M., Fairbrother, A., Gok, A., Ahmad, S., Kazim, S., Lobato, K., Oreski, G., Reinders, A., Schmitz, J., Theelen, M., Yilmaz, P., & Kettle, J. (2022). Review of degradation and failure phenomena in photovoltaic modules. *Renewable and Sustainable Energy Reviews*, *159*, 112160. https://doi.org/10.1016/j.rser.2022.112160

BNEF. (2024, March 4). Global PV Market Outlook—1Q 2024. BloombergNEF. https://about.bnef.com/blog/1q-2024-global-pv-market-outlook/

Czanderna, A. W., & Pern, F. J. (1996). Encapsulation of PV modules using ethylene vinyl acetate copolymer as a pottant: A critical review. *Solar Energy Materials and Solar Cells*, *43*(2), 101-181. https://doi.org/10.1016/0927-0248(95)00150-6

Dintcheva, N. T., Morici, E., & Colletti, C. (2023). Encapsulant Materials and Their Adoption in Photovoltaic Modules: A Brief Review. *Sustainability*, *15*(12), 9453. https://doi.org/10.3390/su15129453

Gok, A., Fagerholm, C. L., French, R. H., & Bruckman, L. S. (2019). Temporal evolution and pathway models of poly(ethylene-terephthalate) degradation under multi-factor accelerated weathering exposures. *PLOS ONE*, *14*(2), e0212258. https://doi.org/10.1371/journal.pone.0212258

Griffini, G., & Turri, S. (2016). Polymeric materials for long-term durability of photovoltaic systems. *Journal of Applied Polymer Science*, *133*(11). https://doi.org/10.1002/app.43080

Hara, K., & Chiba, Y. (2021). Spectroscopic investigation of long-term outdoor-exposed crystalline silicon photovoltaic modules. *Journal of Photochemistry and Photobiology A: Chemistry*, *404*, 112891. https://doi.org/10.1016/j.jphotochem.2020.112891

IEA PVPS. (2023). Snapshot of Global PV Markets 2023 (IEA-PVPS T1-44:2023). International Energy Agency (IEA) Photovoltaic Power Systems Programme (PVPS). https://iea-pvps.org/snapshot-reports/snapshot-2023/

IEA PVPS. (2024). Snapshot of Global PV Markets 2024 (IEA-PVPS T1-42: 2024). International Energy Agency (IEA) Photovoltaic Power Systems Programme (PVPS). https://iea-pvps.org/snapshot-reports/snapshot-2024/

IEC. (2021). IEC 61215-1-1:2021: Terrestrial photovoltaic (PV) modules—Design qualification and type approval—Part 1-1: Special requirements for testing of crystalline silicon photovoltaic (PV) modules (Version 2.0) [International Standard]. International Electrotechnical Commission. https://webstore.iec.ch/publication/61346

ITRPV. (2024). International Technology Roadmap for Photovoltaics. VDMA e. V. https://www.vdma.org/international-technology-roadmap-photovoltaic

Kempe, M. D., Jorgensen, G. J., Terwilliger, K. M., McMahon, T. J., Kennedy, C. E., & Borek, T. T. (2007). Acetic acid production and glass transition concerns with ethylene-vinyl acetate used in photovoltaic devices. *Solar Energy Materials and Solar Cells*, *91*(4), 315-329. https://doi.org/10.1016/j.solmat.2006.10.009

Kempe, M. D., Panchagade, D., Reese, M. O., & Dameron, A. A. (2015). Modeling moisture ingress through polyisobutylene-based edge-seals: Polyisobutylene-based edge-seals. *Progress in Photovoltaics: Research and Applications*, *23*(5), 570-581. https://doi.org/10.1002/pip.2465

Köntges, M., Kurtz, S., Packard, C., Jahn, U., Berger, K. A., Kato, K., Friesen, T., Liu, H., & Van Iseghem, M. (2014). Review of failures of photovoltaic modules (IEA-PVPS T13-01:2014). International Energy Agency (IEA) Photovoltaic Power Systems Programme (PVPS). https://iea-pvps.org/key-topics/review-of-failures-of-photovoltaic-modules-final/

Köntges, M., Oreski, G., Jahn, U., Herz, M., Hacke, P., Weiß, K.-A. Razongles, G., Paggi, M., Parlevliet, D., Tanahashi, T., & French, R. H. (2017). Assessment of photovoltaic module failures in the field (IEA-PVPS T13-09:2017). International Energy Agency (IEA) Photovoltaic Power Systems Programme (PVPS). https://iea-pvps.org/key-topics/report-assessment-of-photovoltaic-module-failures-in-the-field-2017/

Mitterhofer, S., Barretta, C., Castillon, L. F., Oreski, G., Topič, M., & Jankovec, M. (2020). A Dual-Transport Model of Moisture Diffusion in PV Encapsulants for Finite-Element Simulations. *IEEE Journal of Photovoltaics, 10*(1), 94-102. https://doi.org/10.1109/JPHOTOV.2019.2955182

Müller, A., Friedrich, L., Reichel, C., Herceg, S., Mittag, M., & Neuhaus, D. H. (2021). A comparative life cycle assessment of silicon PV modules: Impact of module design, manufacturing location and inventory. *Solar Energy Materials and Solar Cells, 230*, 111277. https://doi.org/10.1016/j.solmat.2021.111277

Oliveira, M. C. C. de, Diniz Cardoso, A. S. A., Viana, M. M., & Lins, V. de F. C. (2018). The causes and effects of degradation of encapsulant ethylene vinyl acetate copolymer (EVA) in crystalline silicon photovoltaic modules: A review. *Renewable and Sustainable Energy Reviews, 81*, 2299-2317. https://doi.org/10.1016/j.rser.2017.06.039

Oreski, G., Stein, J., Eder, G., Berger, K., Bruckman, L., Vedde, J., Weiss, K.-A., Tanahashi, T., French, R., & Ranta, S. (2021). Designing New Materials for Photovoltaics: Opportunities for Lowering Cost and Increasing Performance through Advanced Material Innovations (IEA-PVPS T13-13:2021). International Energy Agency (IEA) Photovoltaic Power Systems Programme (PVPS). https://iea-pvps.org/key-topics/designing-new-materials-for-photovoltaics/

Paç, A. B., & Gok, A. (2024). Assessing the Environmental Benefits of Extending the Service Lifetime of Solar Photovoltaic Modules. *Global Challenges, 8*(8), 2300245. https://doi.org/10.1002/gch2.202300245

Patel, A. P., Sinha, A., & Tamizhmani, G. (2020). Field-Aged Glass/Backsheet and Glass/Glass PV Modules: Encapsulant Degradation Comparison. *IEEE Journal of Photovoltaics, 10*(2), 607-615. https://doi.org/10.1109/JPHOTOV.2019.2958516

Schnatmann, A. K., Schoden, F., & Schwenzfeier-Hellkamp, E. (2022). Sustainable PV Module Design—Review of State-of-the-Art Encapsulation Methods. *Sustainability, 14*(16), 9971. https://doi.org/10.3390/su14169971

Segbefia, O. K., Imenes, A. G., & Sætre, T. O. (2021). Moisture ingress in photovoltaic modules: A review. *Solar Energy, 224*, 889-906. https://doi.org/10.1016/j.solener.2021.06.055

Sinha, A., Sulas-Kern, D. B., Owen-Bellini, M., Spinella, L., Uličná, S., Pelaez, S. A., Johnston, S., & Schelhas, L. T. (2021). Glass/glass photovoltaic module reliability and degradation: A review. *Journal of Physics D: Applied Physics, 54*(41), 413002. https://doi.org/10.1088/1361-6463/ac1462